Journal of Materials Physics and Chemistry, 2022, Vol. 10, No. 1, 1-9
Available online at http://pubs.sciepub.com/jmpc/10/1/1
Published by Science and Education Publishing
DOI:10.12691/jmpc-10-1-1

Theoretical Study on Imidazopyridinyl-chalcones based Dimers Mechanism of Formation Using Quantum Chemistry Methods

Bibata KONATE, Sopi Thomas AFFI*, Doh Soro, Kafoumba BAMBA, Nahossé ZIAO

Laboratoire de Thermodynamique et de Physico-Chimie du Milieu (LTPCM),
Unité de Formation et de Recherche- Sciences Fondamentales et Appliquées (UFR-SFA),
Université NANGUI ABROGOUA (UNA), Abidjan, Côte d'Ivoire
*Corresponding author: affithomas.sfa@univ-na.ci

Received November 01, 2021; Revised December 03, 2021; Accepted December 09, 2021

Abstract Imidazo[1,2-a]pyridinyl-chalcones (IPCs) offer a broad spectrum of biological activities with molecular diversity possible by synthesis. Two potential reactive sites were identified within their basic molecular skeleton from which obtaining dimers by synthesis is possible. In this study, at the level B3LYP/6-311G(d), work focused on elucidating both the mode of bond formation between the two reactive sites and the concerted course of dimerization reaction in the IPC series according to the concepts and tools of transition state theory. Four substituted IPC molecules with stronger nematicidal activity were used in addition to the unsubstituted IPC molecule as monomers. Calculations performed on each initial reactive system modelled using two IPCs led to a unique transition structure in each case. Molecular dimerization in IPC series was found to follow a one-step reaction mechanism. It involved the formation of two covalent bonds, C_5–$C_{14'}$, and C_{14}–$C_{29'}$. The stabilization of the second bond was faster than the first which, moreover, required less energy for establishment. Analysis of bond lengths confirmed the stability of the bonds formed. The energy parameters and the characteristics of the reaction path proved the stability of the dimers envisaged with respect to the reagents used. The path of dimerization reaction in the IPC series was found to be substitution independent but the activation energies depended on the overall nucleophilicity of monomers.

Keywords: *Quantum chemistry, Dimerization, Imidazopyridinyl-chalcone, Reaction mechanism, DFT method*

Cite This Article: Bibata KONATE, Sopi Thomas AFFI, Doh Soro, Kafoumba BAMBA, and Nahossé ZIAO, "Theoretical Study on Imidazopyridinyl-chalcones based Dimers Mechanism of Formation Using Quantum Chemistry Methods." *Journal of Materials Physics and Chemistry*, vol. 10, no. 1 (2022): 1-9. doi: 10.12691/jmpc-10-1-1.

1. Introduction

Chalcones and imidazopyridines almost always exhibit high activity against the responsible germs of many diseases commonly found in developing countries. Imidazo[1,2-a]pyridinyl-chalcones (IPC) therefore have a dynamic profile of biological activities. These hybrid chalcones are susceptible to exert properties of both imidazopyridines and chalcones. Their interesting therapeutic virtues against cancers [1] and bacteria [2] have been reported. IPCs were biologically most remarkable when tested against resistant strains of the nematode, *haemonchus contortus* [3]. Biological potentials coupled with molecular diversity possible by synthesis of IPCs motivate studies of physicochemical characterizations [4,5] and structure-activity relationships [6] in the IPC series. Nematodes live as parasites in humans, animals and plants. Infections caused by these parasites are common and often go unnoticed. Among the factors that exacerbate microbial resistance, there are the misuse and irrationality of drugs. The resulting infections are very often serious and have a huge impact ranging from farms to human health. Drug resistance remains a public health problem that constantly invites to take up several challenges such as research and the development of new molecules, more active and effective against resistant germs. The development of new drug candidates is possible by linking two biologically active pharmacophores from covalent bond [7]. However, the choice of the basic pharmacophores remains decisive for the effectiveness of the desired activity. In this case, the synthetic imidazopyridinyl-chalcone compounds identified for their remarkable nematicidal potentials constitute promising basic entities for the development of new more active nematicidal molecules. Obtaining IPC dimers is therefore a path that deserves special attention in strategies for the discovery and development of new therapeutic agents that may be more effective and less toxic. In a recent theoretical study on chemical reactivity of an IPC series [8], the preferred sites of reactivity were identified within their basic molecular skeleton. Respectively, the carbon atom from imidazopyridine nucleus directly linked

to carbonyl carbon and the β-carbon atom from ceto-ethylenic linker were identified as the sites of electrophilic attacks and nucleophilic attacks. The nucleophilicity and electrophilicity characters of these reactive centres were found to be not substituent-dependent. Additionally, the study revealed that IPCs can be both electron donors and acceptors. These characteristics of the overall reactivity of IPCs were influenced by the substituent on aryl ring. However, for the chemist, the implementation of any reaction requires knowledge of the sequence of steps which describe through which reaction intermediates and through which transition states the reactants lead to the products In general, this work is a theoretical study which aims first to determine the concerted course of the molecular dimerization in the IPC series and then to understand the formation of the bond involving the preferred reactive sites predicted in the previous study [8]. This could open another way of synthesizing new molecules but also provide access to a new source of molecules with possibly improved biological properties. In this area, the tools of quantum chemistry and the theories of chemical reaction are of great help. Determining the characteristics of the reactants, products, intermediates and transition states as well as those of the reactions will help to understand how the reactants have evolved in relation to each other until the products were obtained. The envisaged reaction consists of establishing a covalent bond involving the electrophilic and nucleophilic attack sites identified in the skeleton of IPCs. These are the C_5 nucleophilic site located in the nucleophilic monomer M and the electrophilic site C_{14}', located in the electrophilic monomer M' (Figure 1). There are five IPC derivatives taken as basic monomers in this study. The structures and the systematic nomenclature of these compounds are presented in Table 1. The reference codes of the molecules, formed by the acronym "IPC" to translate "imidazopyridinyl-chalcone" followed by a number which gives the order of its selection, are also indicated.

Table 1. Molecular structures of IPC derivatives used as monomers for the dimerization reaction

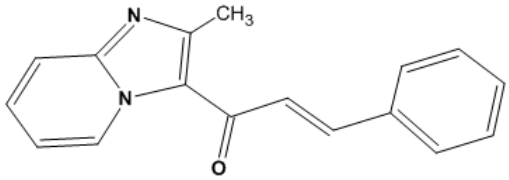 1-(2-methylimidazo[1,2-*a*]pyridin-3-yl)-3-phenylprop-2-en-1-one (**IPC-1**)
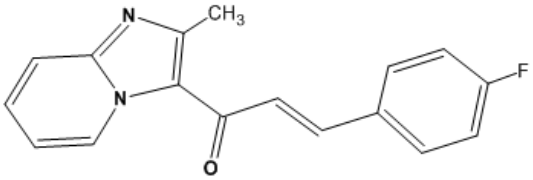 3-(4-fluorophenyl)-1-(2-methylimidazo[1,2-*a*]pyridin-3-yl)prop-2-en-1-one (**IPC-2**)
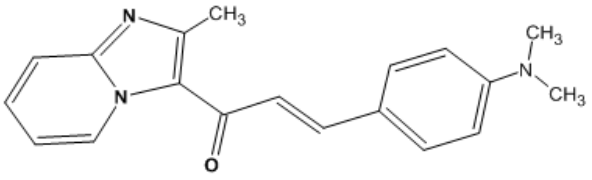 3-[4-(dimethylamino)phenyl]-1-(2-methylimidazo[1,2-*a*]pyridin-3-yl)prop-2-en-1-one (**IPC-3**)
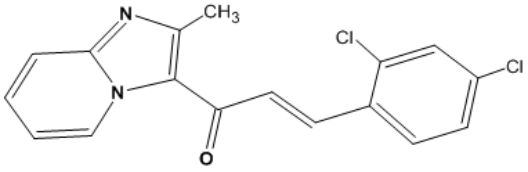 3-(2,4-dichlorophenyl)-1-(2-methylimidazo[1,2-*a*]pyridin-3-yl)prop-2-en-1-one (**IPC-4**)
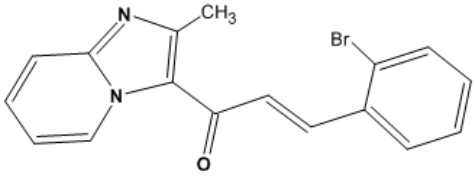 3-(2-bromophenyl)-1-(2-methylimidazo[1,2-*a*]pyridin-3-yl)prop-2-en-1-one (**IPC-5**)

These molecules differ in the nature and/or the position of the substituent of the aryl group. The substituted molecules, IPC-2, IPC-3, IPC-4 and IPC-5, were shown to be more nematicidal than the reference drugs. The selection of the parent molecule IPC-1 will allow consideration of the substitution effect on the dimerization process.

2. Computational Details

Figure 1 shows the reactive system with highlighted reactivity sites as well as some atoms which are linked to them. This reaction scheme leads to the production of homodimers. These products are coded by D_{i-i} where "i" reflects the selection order of the monomer IPC. Thus, D_{1-1}, D_{2-2}, D_{3-3}, D_{4-4}, D_{5-5} will identify the dimers obtained with IPC-1, IPC-2, IPC-3, IPC-4 and IPC-5, respectively. Gaussian09 [9] was used to perform all calculations and GaussView for modelling and visualizing the chemical structures. DFT method and its hybrid functional B3LYP were employed with the basis set 6-311G(d) for geometry optimization as well as frequencies calculations. These types of calculation jobs not only allow access to the thermochemical and vibrational parameters of the studied systems, but also to determine the nature of each stationary state of reaction. The ground state of any reactant and any product is verified by the absence of any imaginary frequency unlike any transition structure which is characterized by the presence of a single imaginary frequency in the Hessian matrix.

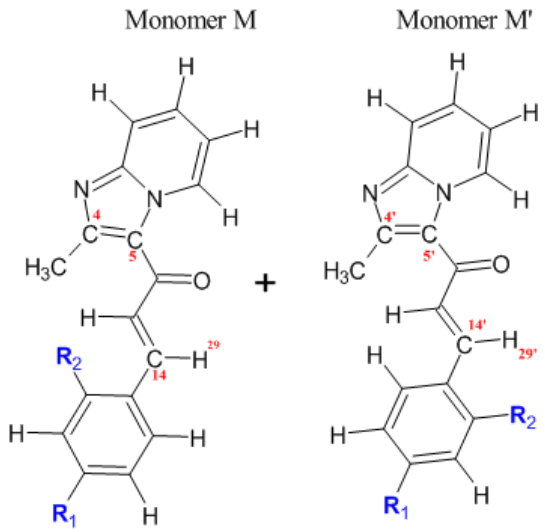

Figure 1. Illustration of the initial reactive system for dimerization process envisaged on the basis of IPC monomers

Knowledge of the transition state is crucial in studying the mechanism of a reaction [10]. Several research methodologies exist. The STQN (*Synchronous Transit-Guided Quasi-Newton*) methods developed and implemented by Schlegel *et al*. [11,12] in the Gaussian program are very useful in locating transition states. The QST2 (Quadratic Synchronous Transition) option was used. It requires the specification of the reagents and product, previously optimized, as entries, in the same order. The initial arrangement of reagents is made based on the extension of Hammond's postulate. According to this postulate, if two successive states on a reaction path are close then their interconversion requires only a slight modification of structure. Thus, the geometries of the reactants are initialized taking into account the configuration of the corresponding dimers while separating the reactive sites at a distance of 3 Å. A frequency calculation is performed on the geometry of the transition state obtained by the QST2 calculation in order to verify the presence of the imaginary frequency. Likewise, in order to ensure that the reaction is well concerted, an IRC (Intrinsic Reaction Coordinates) calculation is performed to find the minimum energy path passing through this transition state. It is important to note that the modifications of the geometries of the reagents cannot call into question the transition structures since they are part of strategies of reagents orientation in the direction of efficient collisions. Also, for a chemical reaction to occur upon collision, the reactive compounds must have a required minimum amount of energy. This energy called activation energy E_a is calculated following the relation:

$$E_a = E_{ts} - E_R$$

with E_R as the reactants energy and E_{TS} as the transition state energy.

On the other hand, reactions without solvent are less common in practice. The solvents act as a support in the chemical reaction and possibly allow the reagents to dissolve in order to homogenize the reaction mixture. Calculations are also carried out in the presence of solvents such as water and ethanol (polar protic), dimethyl sulfoxide (DMSO, polar aprotic) and benzene (nonpolar aprotic). The solvation effects were taken into account using the PCM model [13-17].

3. Results and Discussion

All the calculations of frequency which followed those of the geometry optimization of the monomers and dimers resulted in the confirmation of their respective ground state. The optimized structures of monomers and dimers are shown in Figure 2 and Figure 3, respectively.

3.1. Characteristics of Localized Transition States

The optimization and frequency calculations carried out on each transition structure from the QST2 calculations, in the gas model, resulted in the presence of an imaginary frequency of -1300cm^{-1}, in the Hessian matrix. Thus, the obtained geometry configurations correspond to the transition states leading to formation of the corresponding dimers. Animation of this structure using GaussView software made it possible to observe that this imaginary frequency of vibration involved the balancing of the

hydrogen atom H_{29}' between the carbon atom C_4 of monomer M and the carbon atom C_{14}' of monomer M' (Figure 4).

Visualization of the transition structures revealed the formation of new bonds and a breaking of bond between atoms. Geometry and energy characteristics of the different transition structures corresponding respectively to dimers D_{1-1} , D_{2-2} , D_{3-3} , D_{4-4} and D_{5-5} were determined and then analysed.

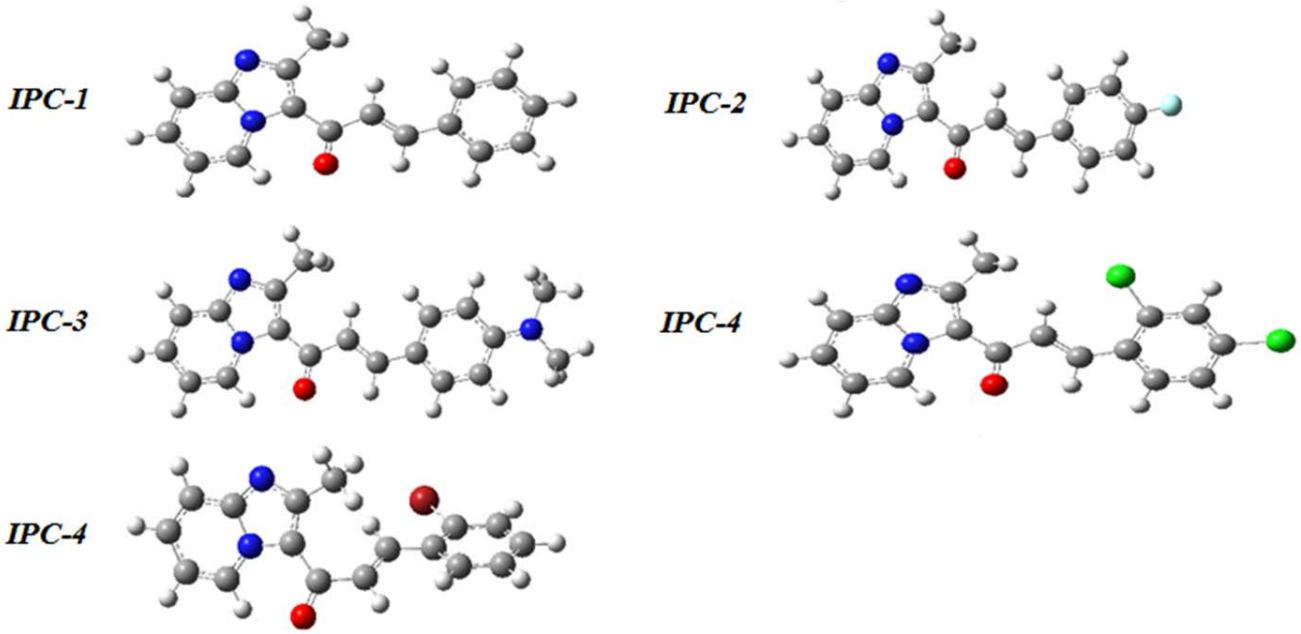

Figure 2. Optimized structures of IPC molecules obtained at the B3LYP / 6-311G level (d)

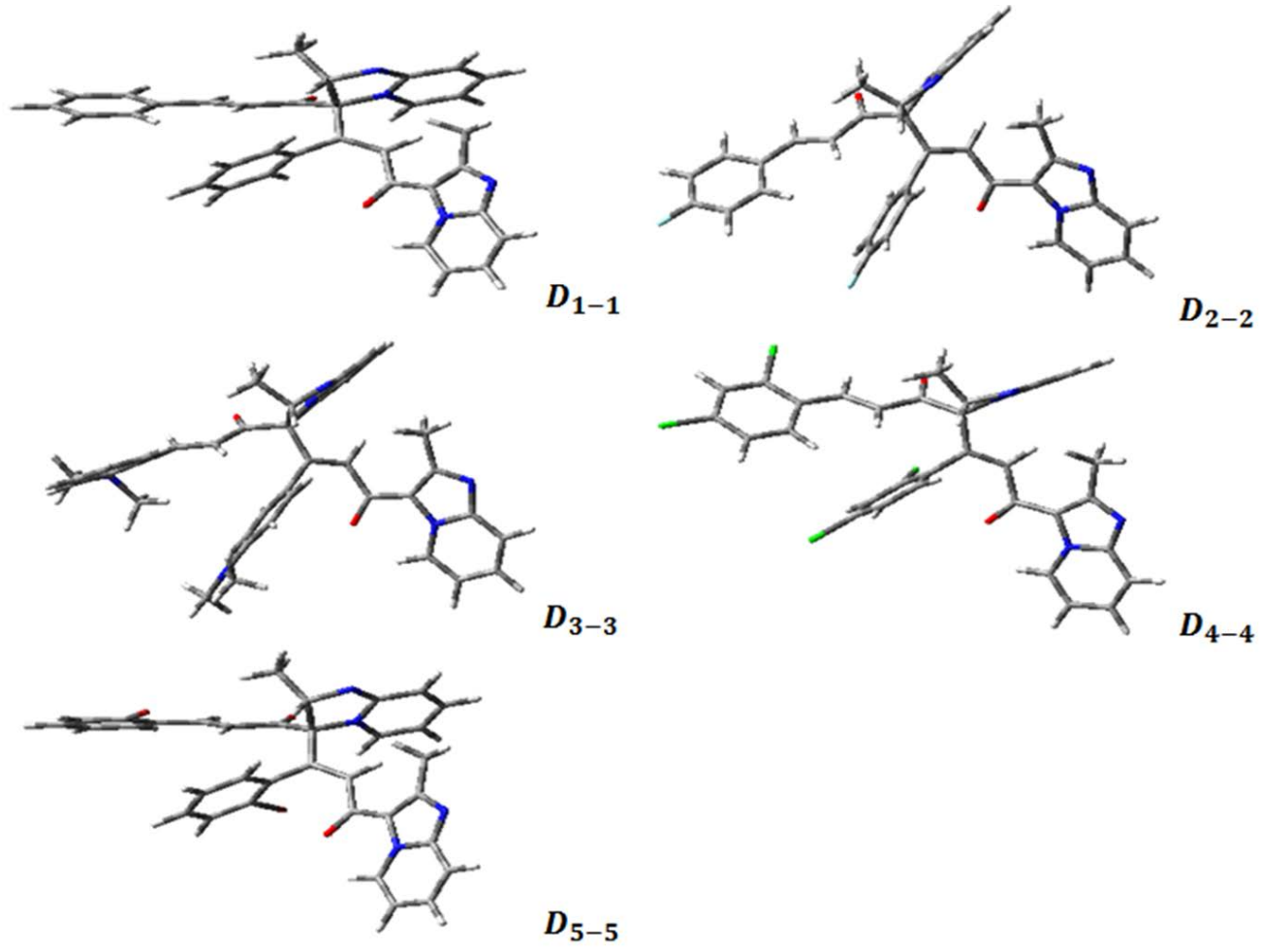

Figure 3. Optimized structures of dimers at the theory level B3LYP / 6-311G (d)

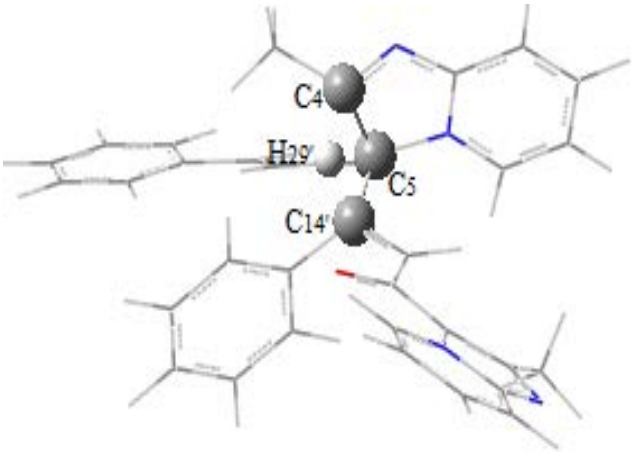

Figure 4. Structure of the transition state showing the two links corresponding to the vibration mode

3.1.1. Analysis of the Geometry Characteristics

The distances between the atoms involved, on the one hand, in the formation of bonds (C_5 and $C_{14'}$; C_4 and $H_{29'}$) and on the other hand, in the breaking of the bond ($C_{14'}$ and $H_{29'}$), along the reaction path, are shown in Table 2.

Table 2. Characteristic bond lengths (in Å) in stationary states along the dimerization path, determined at the B3LYP / 6-311G (d) level, in vacuum

Dimers	Bonds	Reagents	Transition States	Products
		Distances (in Angstroms)		
D_{1-1}	$C_5 - C_{14'}$	3.0000	1.5936	1.5545
	$C_{14'} - H_{29'}$	1.0700	1.3145	2.5984
	$C_4 - H_{29'}$	2.4730	1.4736	1.0915
D_{2-2}	$C_5 - C_{14'}$	3.0000	1.5937	1.5553
	$C_{14'} - H_{29'}$	1.0700	1.3147	2.6120
	$C_4 - H_{29'}$	2.4730	1.4753	1.0912
D_{3-3}	$C_5 - C_{14'}$	3.0000	1.5967	1.5559
	$C_{14'} - H_{29'}$	1.0700	1.3123	2.6111
	$C_4 - H_{29'}$	2.4730	1.4711	1.0912
D_{4-4}	$C_5 - C_{14'}$	3.0000	1.5970	1.5512
	$C_{14'} - H_{29'}$	1.0700	1.3230	2.5635
	$C_4 - H_{29'}$	2.4730	1.4598	1.0930
D_{5-5}	$C_5 - C_{14'}$	3.0000	1.5978	1.5522
	$C_{14'} - H_{29'}$	1.0700	1.3193	2.5742
	$C_4 - H_{29'}$	2.4730	1.4625	1.0928

All the interatomic distances noted in this table have undergone variations from the initialization in the reagents to the products through the transition states. From one dimer to another, the distance at initialization between atoms C_5 and $C_{14'}$ (3.000 Å) decreased to final values of between 1.551 Å — 1.556 Å, at the product level. Observation is identical between atoms C_4 and $H_{29'}$ where the initial distance which separated them went from 2.473 Å to final distances of 1.091 Å — 1.093 Å. This rapprochement, which has taken place up to these final distances at the product level, defined the conditions for the formation of covalent bonds between atoms. Indeed, in the dimers, the lengths of the $C_5 - C_{14'}$ bond are almost equal to the experimental length of a single bond $C - C$. Concerning the formation of the covalent bond $C_4 - H_{29'}$, the hydrogen $H_{29'}$ began by moving away from the $C_{14'}$ carbon by a distance of 1.070 Å in the reactants. This distance practically reached the distance of 2.6 Å in the products. This length (2.6 Å) is abnormally long when compared to the experimental length of the covalent bond $C - H$ approximately equal to 1.09 Å. Thus, the hydrogen atom $H_{29'}$ is totally disconnected from the carbon $C_{14'}$ and approached the carbon C_4 at the distance of 1.09 Å, close to the experimental value of a single bond $C - H$. Therefore, from the point of view of formed bonds lengths, the reaction involving two monomers IPC resulted in a dimer by the connection of carbon atoms C_5 and $C_{14'}$. Furthermore, in the characterization of a chemical reaction, the prediction of effectiveness or even speed and stability of the final products is important. At this level, the energy characteristics are of great interest in studying the evolution of the reactive system until the products are obtained.

3.1.2. Analysis of Energy Characteristics

In Table 3, the energies of the reactants (E_R), of the transition state (E_{TS}) and of the products dimer (E_P) which made it possible to calculate the activation energy (E_a) and the reaction free enthalpy ($\Delta_r G^0_{298}$) are together presented.

Table 3. Energy characteristics of stationary states along the path of dimer formation determined at the B3LYP / 6-311G (d) level, in vacuum (E_R, E_{TS} and E_P were evaluated in a.m.u. (atomic mass unity) while E_a and $\Delta_r G^0_{298}$ were evaluated in kcal/mol)

Dimers	E_R	E_{TS}	E_P	E_a	$\Delta_r G^0_{298}$
D_{1-1}	-1682.1991	-1682.1683	-1682.2285	19.3270	-18.4485
D_{2-2}	-1888.7305	-1888.7001	-1888.7603	19.0760	-18.6995
D_{3-3}	-1950.1941	-1950.1644	-1950.2232	18.6367	-18.2602
D_{4-4}	-3520.6839	-3520.6527	-3520.7115	19.5780	-17.3190
D_{5-5}	-6829.2740	-6829.2435	-6829.3025	19.1387	-17.8837

All the values of the activation energy E_a related to the formation of dimers (D_{1-1}, D_{2-2}, D_{3-3}, D_{4-4} and D_{5-5}) are between 18.64 kcal/mol and 19.58 kcal/mol. By definition, activation energy is the least amount of energy required to activate atoms or molecules to a state in which they can undergo a chemical reaction. It is therefore an energy parameter that can be associated with the speed with which a reaction takes place. In other words, when the activation energy is low the transition state is quickly reached and the process of obtaining the final product is triggered earlier. The low activation energy (18.6367 kcal/mol) is obtained when two monomers IPC-3 reacted. The high activation energy (19.5780 kcal/mol) is due to the reaction of the monomers IPC-4. Therefore, the process to obtain the dimer D_{3-3} could start earlier while that to obtain the dimer D_{4-4} would require an additional energy of 0.94125 kcal/mol compared to the first. By the way, IPC-3 and IPC-4 have been found to be, respectively, the most nucleophilic and electrophilic molecules [8]. The sequence of evolution defined according to the increasing order of the activation energy values was as follows:

$$E_a : D_{3-3} < D_{2-2} < D_{5-5} < D_{1-1} < D_{4-4}$$

This sequence of activation energy evolution is opposed to that of the overall nucleophilicity established with these nematicidal molecules IPC-2, IPC-3, IPC-4 and IPC-5 [8]. The dimerization activation energy is therefore high when

the overall nucleophilicity of the substituted monomer IPC is low. Under these conditions, any substitution by a strong electron-donor group proves to be favourable to the fast activation of the process for obtaining dimers. Free enthalpies also give information about the spontaneity of a reaction and the stability of the obtained product. In Table 3, all the values of the dimerization free enthalpy are negative: the obtaining of dimers envisaged from the IPC monomers, at 298 K under 1 atm, is possible and spontaneous at the level B3LYP/6-311G(d), in the gaseous medium. Moreover, the negative sign of the $\Delta_r G^0_{298}$ values reflects that the reactants are very high in energy compared to the products; under these conditions, the products are found more stable than the starting reagents. Thus, whatever the envisaged dimerization reaction, the dimer obtained is always more stable than the monomers put together.

3.2. Analysis of the Evolution Curve of the Dimerization Reaction

Generally speaking, the energy profile of a reaction is used to track the energy evolution of the reacting system from monomers IPC to dimers based IPC as a function of an intrinsic reaction coordinate. Figure 5 is used to illustrate the energy profiles corresponding to obtaining homodimers ($D_{1\text{-}1}$, $D_{2\text{-}2}$, $D_{3\text{-}3}$, $D_{4\text{-}4}$ and $D_{5\text{-}5}$) , respectively.

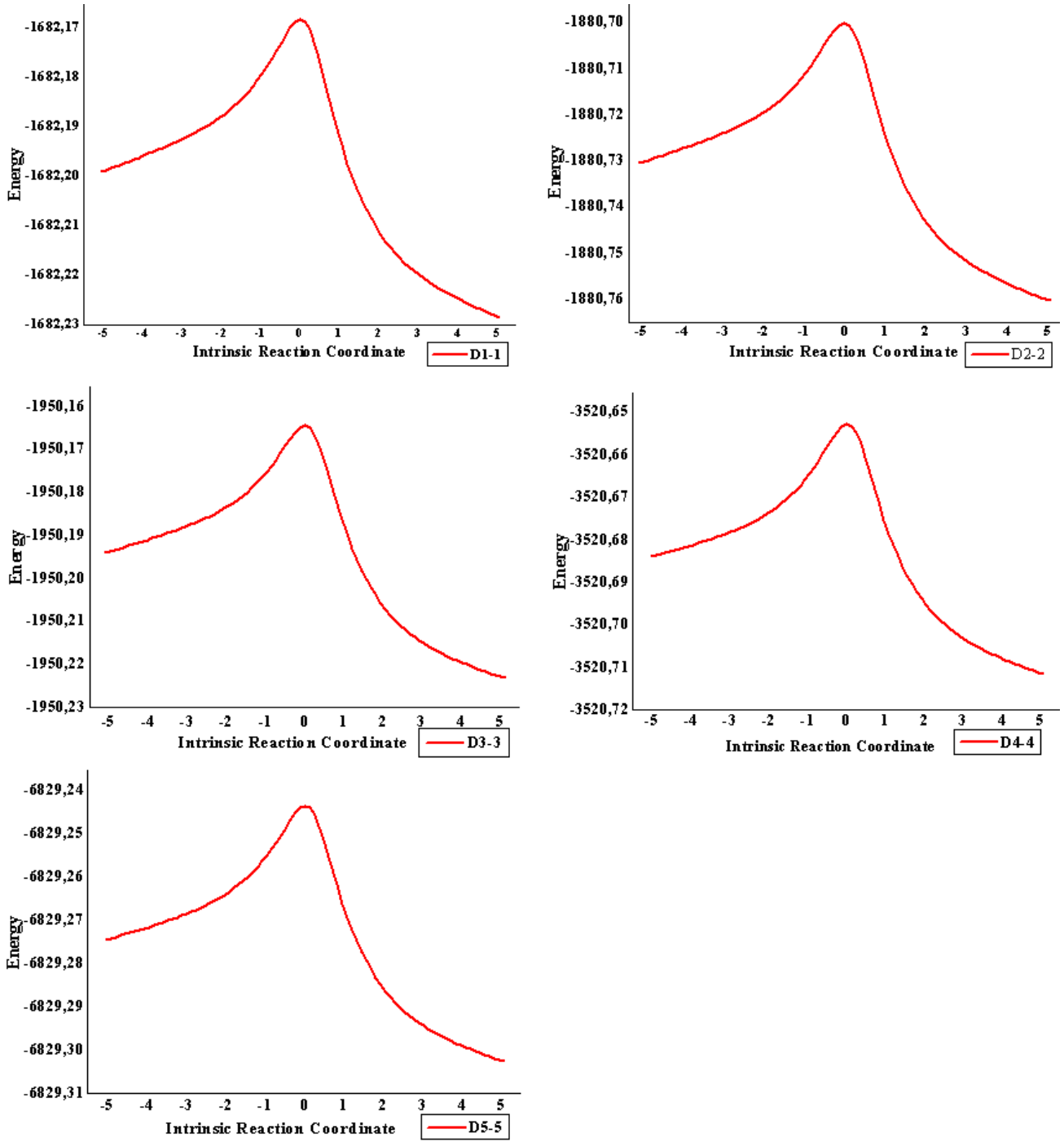

Figure 5. Curves of the reaction paths of the homodimers studied obtained at the level of theory B3LYP / 6-311G (d) according to the QST2 approach

By observing these energy profiles for obtaining the homodimers envisaged, we note the presence of a single maximum and two distinct minima at each curve regardless of the starting monomers. The highest minimum in energy is that of the initial reactive system and the lowest minimum in energy is that of the final product. Each maximum corresponds to the transition state of the process of obtaining the dimer. The position of the minimum of the reactive system relative to the minimum of the final product clearly shows the stability of the dimers obtained relative to the starting monomers. Thus, the maximum of the transition state in relation to the minima of the reagents and the products translates to obtaining the IPC dimers in a single step. IPC series dimerization is therefore an elementary reaction. On the other hand, although the energies corresponding to the optimum points differ from one dimerization process to another, the energy profiles show the same pace of evolution. Therefore, the mechanism for obtaining IPC dimers would involve the same chemical phenomena regardless of the IPC monomers used. The chemical phenomena involved in a reaction mechanism can be demonstrated through the curve of the mean squares along the reaction path. Examining the variations shown by the RMS gradient along the IRC curve is therefore a sensitive and useful tool that helps identify regions along the reaction path where the main chemical events occur. In this work, the reaction path was followed by performing an IRC calculation with 42 points of interest on either side of the transition state. This is to highlight the 42 major structural changes that take place along the way, from reactants to the transition state, as well as from the transition state to the product. A representation of the root-mean-square gradient for the D_{1-1} dimer-obtaining reaction along the intrinsic coordinate of the reaction is shown in Figure 6.

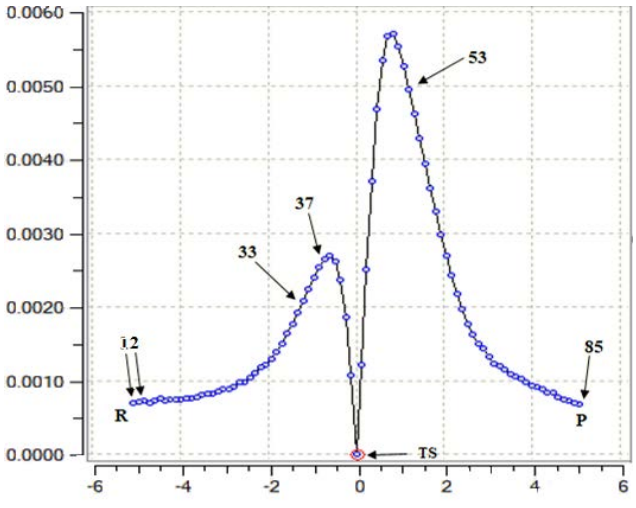

Figure 6. Curve of RMS gradient norms along the dimerization path as a function of intrinsic coordinates

The RMS curve obtained using Gaussian software has two parts. The negative part of the intrinsic coordinates is the domain of the changes undergone from the reactive system in the transition state when the positive part concerns the changes undergone from the transition state to the product. On the curve of the RMS gradient standards, the marker numbers ranging from 1 to 43 are associated with the path of the reagents from R (point 1, initial state) to the transition state TS (point 43) when the markers ranging from 43 at 85 are associated with the path from TS to the product at P (point 85, final state), of dimerization. The visualization of the different configurations of the reactive system modelled along the reaction path using the GaussView software made it possible to note some points corresponding to phenomena of structural reorganization. The relative positions of the selected points along the reaction path are shown on the RMS curve. In addition to this curve, Figure 8 reveals the variations of the interatomic distances associated with atoms $\boldsymbol{C_5}$ and $\boldsymbol{C_{14'}}$ then $\boldsymbol{C_4}$ and $\boldsymbol{H_{29'}}$, respectively.

- The activation barrier, represented by the region from points 1 to 43, contains structural and electronic modification events. It occurs in this region:
  - breaking the π bond between the $\boldsymbol{C_5}$ and $\boldsymbol{C_4}$ atoms of the nucleophilic monomer resulting in a single bond between these two atoms when moving from point 1 to point 2 on the reaction path. This event, which occurs early in activation, is likely due to electronic delocalization in favor of nucleophilic activation of the $\boldsymbol{C_5}$ site;
  - the establishment of the bond between atoms $\boldsymbol{C_5}$ and $\boldsymbol{C_{14'}}$ from point 33 for an energy close to 10 kcal / mol supplied to the reactive system.
  - and breaking the $\boldsymbol{C_{14'} - H_{29'}}$ bond at point 37 for near 15.5 kcal/mol energy input to the reactants. The breaking of this bond is a consequence of the establishment of the bond between atoms $\mathbf{C_5}$ and $\mathbf{C_{14'}}$ which occurs just at point 33 on the reaction path.
- The region of points 43 to 85 represents the path of deactivation of the activated complex for the formation of the reaction product. The main event that occurs in this region is the formation of the bond between the $\mathbf{C_4}$ and $\mathbf{H_{29'}}$ atoms, which begins to form from point 53 when the deactivation energy tends to 19 kcal / mol.

3.3. Analysis of the Sequence of Chemical Events of Dimerization

Monitoring the evolution of the distances of the bonds formed (Figure 7; Figure 8) makes it possible to get an idea of the sequence of chemical events that have occurred and then to identify the most decisive during the reaction.

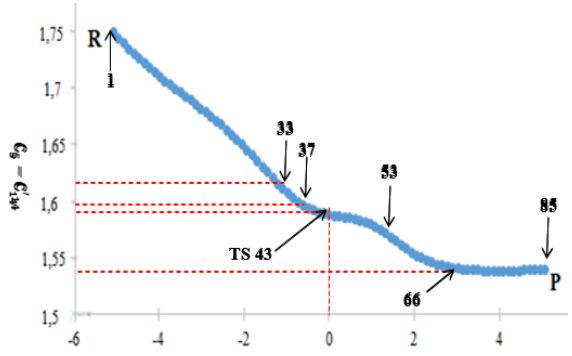

Figure 7. Evolution curve of the interatomic distance of the C_5-$C_{14'}$ bond during the formation of the IPC dimer

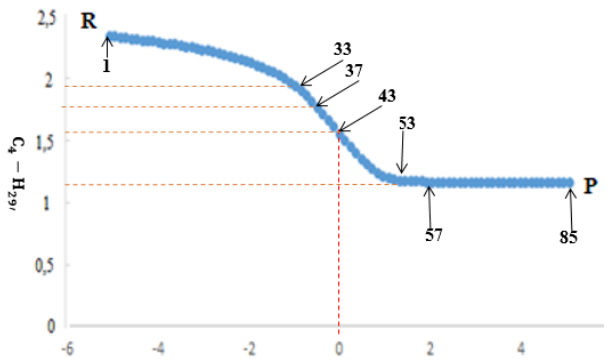

Figure 8. Evolution curve of the interatomic distance of the C_4-$C_{29'}$ bond during the formation of the IPC dimer.

Each curve presents two distinct trends of evolution: a part of monotonic decrease and a plateau. Regarding the evolution of the length of the $\mathbf{C_5 - C_{14'}}$ bond, we note a faster approximation of the two atoms between points 1 and 37 then a slowing down to point 66 from which a plateau is recorded. In the case of the $\mathbf{C_4 - H_{29'}}$ bond, the approximation of the atoms becomes very rapid from point 33 to point 53 where we observe an almost constant evolution opening onto a plateau from point 57. The different plateaus observed characterize the stabilization of bonds in formation. Under these conditions, the $\mathbf{C_4 - H_{29'}}$ bond stabilizes before the $\mathbf{C_5 - C_{14'}}$ bond during the obtaining of dimers. Also, the migration of the hydrogen atom $\mathbf{H_{29'}}$ resulting from the rupture at point 37 to the $\mathbf{C_4}$ atom is faster than the migration to each other of the carbon atoms $\mathbf{C_5}$ and $\mathbf{C_{14'}}$ whose the connection establishment takes place at point 33 of the reaction path. Consequently, the formation of the $\mathbf{C_5 - C_{14'}}$ bond constitutes the determining chemical phenomenon of dimerization. Across the entire reaction mechanism, activating the bonding between $\mathbf{C_5}$ and $\mathbf{C_{14'}}$ requires less energy than activating the breaking of the $\mathbf{C_{14'} - H_{29'}}$.bond.

3.4. Effects of Solvation on the IPC Series Dimerization Reaction

Taking into account the similarity of the energy profiles and, consequently, the mechanism for obtaining probably identical dimers, the prediction study on the solvation of the reaction medium was undertaken by focusing only on obtaining the dimer $\boldsymbol{D_{1-1}}$. At the end of the frequency calculation which followed that of the optimization of the reactive system, a single imaginary frequency in the Hessian matrix was observed, thus confirming that a transition state was obtained in each solvent. The lengths (in Å) of the characteristic bonds observed at the level of the $\boldsymbol{D_{1-1}}$ dimer product were determined in water, ethanol, DMSO and benzene. The different values obtained, in the case of each bond, are given in the order of the solvents used, as follows:

- $C_5 - C_{14'}$: 1.541, 1.542, 1.542 et 1.544 ;
- $C_4 - H_{29'}$: 1.093, 1.094, 1.096 et 1.090 ;

The length of the $C_5 - C_{14'}$ bond formed in the D_{1-1} dimer is almost equal to the experimental length of a single $C - C$ bond (1.552 Å), regardless of the solvent. The same observation is made with the length of the $C_4 - H_{29'}$ bond which is close to the experimental value 1.09 Å of a $C - H$ bond. The energy values relating to the stationary states along the formation path of dimer D_{1-1} are presented in Table 4.

Table 4. Energy characteristics of stationary states along the path of D_{1-1} dimer formation determined at the B3LYP6-311G (d) level, in solvents (E_R, E_{TS} and E_P were evaluated in a.m.u. (atomic mass unity) while E_a and $\Delta_r G^0_{298}$ were evaluated in kcal/mol)

Solvent	E_R	E_{TS}	E_P	E_a	$\Delta_r G^0_{298}$
Eau	-1682.2290	-1682.1675	-1682.2995	38.5912	-0.3137
Ethanol	-1682.2290	-1682.1676	-1682.2294	38.5285	-0.2510
DMSO	-1682.2290	-1682.1675	-1682.2295	38.5912	-0.3137
Benzene	-1661.9372	-1661.8284	-1661.9380	68.2720	-0.5020

When analysing the values in the table, the reactants and the products are practically at the same level of energy, whatever the solvent. The dimer D_{1-1} however remains lower in energy than the reactive system with a maximum difference between the values of 0.001 a.m.u, or 0.6275 kcal/mol observed in the case of water. Also, from one polar solvent to another, the energies corresponding to the reactive system, to the transition state, to the product and to the reaction activation are of the same order of magnitude, respectively. For example, activation energy values range from 38.5285 to 38.5912 kcal/mol. Moreover, all of these energy values observed in the case of polar solvents remain lower than those obtained with the non-polar solvent, benzene. At the level of stationary states, the maximum deviation is 20.33 a.m.u or 12757.07 kcal/mol when at the level of activation energy, the maximum deviation reaches the value 29.74 kcal/mol. This demonstrates the influence of the polarity of solvents on the dimerization process. The lower activation energy observed in the case of polar solvents, however, reflects the easy reaction of IPC1 monomers in this medium. In terms of the variations in the free enthalpy of the reaction, they are all negative ($\Delta_r G^0_{298} < 0$) indicating the possibility of spontaneously obtaining the D_{1-1} dimer regardless of the polar nature of the solvent used. The value obtained for benzene is still very low compared to the values obtained using water, ethanol and DMSO. Also, the negative sign of the free enthalpy of reaction indicates the great stability of the dimer compared to that of the reagents used, in the various media. Considering the energetic characteristics, on the one hand, of the stationary states and of the activation barrier and then on the other hand, of the reaction, we can say that the non-polar solvent is favourable to the stabilization of the dimer formed and the polar solvents them environments, favourable to the rapid initiation of the reaction. At the same time, it is noted that the characteristic energies of the stationary states and of the reaction are all higher in the solvents than in the gas phase. This predicts a faster IPC serial dimerization reaction with more stable dimers in the gas phase than in solvents. Also, the rarity of reactions without solvent, would invite to explore the mixture of an apolar solvent (benzene) with a miscible polar solvent (ethanol, DMSO) thus making it possible to predict not only the rapid initiation of the reaction but also the stability of the desired product.

4. Conclusion

The study of dimer formation was conducted using quantum chemistry methods at the level of theory B3LYP/6-311G(d). Thermodynamic characteristics predicted the possible formation and existence of the designed dimers at temperature of 298.15 K and pressure of 1 atm. Applying transition state theory and using IRC curves made it possible to identify: ─ the presence of a single activated complex which brings into play the hydrogen atom linked to the β-carbon in the electrophilic monomer ; ─ a single-step mechanism where the breaking of the $\boldsymbol{C_{14'} - H_{29'}}$ bond, and the formation of new $\boldsymbol{C_5 - C_{14'}}$ then $\boldsymbol{C_4 - H_{29'}}$ bonds were carried out in a concerted manner; ─ the stability of the IPC dimers envisaged compared to the basic IPC monomers. The prediction study of the solvent to be considered made it possible to note the polar effects on the activation of the reaction and on the stabilization of the obtained dimer products. Various results and observations were noted in this work. They constituted an important theoretical basis in the orientation and implementation of the IPC-based dimer synthesis strategy. Implementation of the synthesis will lead to new sources of molecules whose possible biological tests could reveal their probable therapeutic advantages.

Acknowledgements

The heading of the Acknowledgment section and the References section must not be numbered.

References

[1] Kuthyala, S., Nagaraja, G.K., Sheik, S., Hanumanthappa, M. and Kumar, M.S. Synthesis of Imidazo[1, 2-a]pyridine-chalcones as Potent Inhibitors against A549 Cell Line and Their Crystal Studies, Journal of Molecular Structure 1177, 381-390, September 2018.

[2] Rao, N.S., Kistareddy, C., Balram, B. and Ram, B. Synthesis and Antibacterial Activity of Novel Imidazo[1,2-a]pyrimidine and Imidazo[1,2-a]pyridine Chalcones Derivatives. Der Pharma Chemica 4, 2408-2415, January 2012.

[3] Sissouma, D., Ouattara, M., Koné, M.W., Menan, H.E., Adjou, A. and Ouattara, L. Synthesis and in Vitro Nematicidal Activity of New Chalcones Vectorised by Imidazopyridine. Africa Journal of Pharmacy and Pharmacology, 5, 2086-2093. October, 2011.

[4] Thomas, A.S., Nahossé, Z. and Kafoumba, B. Determination, par des méthodes ab initio et DFT, des sites et énergies de protonation d'une série de molécules d'imidazopyridinyl-chalcones substituées. European Scientific Journal,11, 148-158, November 2015.

[5] Affi, T.S., Ziao, N., Ouattara, M., Sissouma, D. and Yapo, K) Caractérisation théorique des sites d'interaction par liaison hydrogène de 3-(4-isopropylphenyl)-1-(2-méthylimidazopyridin-3-yl)prop-2-en-1-one et de 3-(2-méthoxyphenyl)-1-(2-méthylimidazopyridin-3-yl)prop-2-en-1-one. European Journal of Scientific Research,123, 340-347, June 2014.

[6] Gadkari, S., Choudhari, P., Bhatia, M., Khetmar, S. and Jadhav, S. 3D QSAR, Pharmacophore Identification Studies on Series of Imidazopyridine Analogs as Nematicidal Activity. Pharmacophore, 3, 199-208, 2012.

[7] B. Meunier, "Les molécules hybrides comme stratégie de création de nouveaux agents anti-infectieux," Comptes Rendus Chim., vol. 14, no. 4, pp. 400-405, March 2011.

[8] B. Konate, S. T. Affi, and N. Ziao, "DFT Study of Dimerization Sites in Imidazo [1, 2-a] pyridinyl-chalcone Series," pp. 1-17, December 2020.

[9] Frisch, M.J., Trucks, G.W., Schlegel, H.B., Scuseria, G.E., Robb, M.A., Cheeseman, J.R., Scalmani, G., Barone, V., Mennucci, B., Petersson, G.A., Nakatsuji, H., Caricato, M., Li, X., Hratchian, H.P., Izmaylov, A.F., Bloino, J., Zheng, G., Sonnenberg, J.L., Hada, M., Ehara, M., Toyota, K., Fukuda, R., Hasegawa, J., Ishida, M., Nakajima, T., Honda, Y., Kitao, O., Nakai, H., Vreven, T., Montgomery Jr., J.A., Peralta, J.E., Ogliaro, F., Bearpark, M., Heyd, J.J., Brothers, E., Kudin, K.N., Staroverov, V.N., Kobayashi, R., Normand, J., Raghavachari, K., Rendell, A., Burant, J.C., Iyengar, S.S., Tomasi, J., Cossi, M., Rega, N., Millam, J.M., Klene, M., Knox, J.E., Cross, J.B., Bakken, V., Adamo, C., Jaramillo, J., Gomperts, R., Stratmann, R.E., Yazyev, O., Austin, A.J., Cammi, R., Pomelli, C., Ochterski, J.W., Martin, R.L., Morokuma, K., Zakrzewski, V.G., Voth, G.A., Salvador, P., Dannenberg, J.J., Dapprich, S., Daniels, A.D., Farkas, O., Foresman, J.B., Ortiz, J.V., Cioslowski, J. and Fox, D. J.(2009) Gaussian 09, Revision A.1. Gaussian Inc., Wallingford.

[10] H. Eyring, "The Activated Complex in Chemical Reactions," J. Chem. Phys., vol. 3, no. 2, pp. 107-115, November 1934.

[11] S. H. B. Chunyang P., "Combining ST and QN Methods to Find Transition States," Isr. J. Chem., vol. 33, pp. 449-454, July 1993.

[12] C. Peng, P. Y. Ayala, H. B. Schlegel, and M. J. Frisch, "to Optimize Equilibrium Geometries and Transition States," J. Comput. Chem., vol. 17, no. 1, pp. 49-56, January 1996.

[13] V. Barone, M. Cossi, and J. Tomasi, "A new definition of cavities for the computation of solvation free energies by the polarizable continuum model," J. Chem. Phys., vol. 107, no. 8, pp. 3210-3221, May 1997.

[14] E. Cancès, B. Mennucci, and J. Tomasi, "A new integral equation formalism for the polarizable continuum model: Theoretical background and applications to Isotropic and anisotropic dielectrics," J. Chem. Phys., vol. 107, no. 8, pp. 3032-3041, May 1997.

[15] M. Cossi, V. Barone, R. Cammi, and J. Tomasi, "Ab initio study of solvated molecules: A new implementation of the polarizable continuum model," Chem. Phys. Lett., vol. 255, no. 4-6, pp. 327-335, Fabruary 1996.

[16] M. Cossi, G. Scalmani, N. Rega, and V. Barone, "New developments in the polarizable continuum model for quantum mechanical and classical calculations on molecules in solution," J. Chem. Phys., vol. 117, no. 1, pp. 43-54, April 2002.

[17] J. Tomasi and M. Persico, "Molecular Interactions in Solution : An Overview of Methods Based on Continuous Distributions of the Solvent An Overview of Different Approaches to," pp. 2027-2094, August 1994.